Predicting Relative Binding Affinity Using Nonequilibrium QM/MM Simulations

Wang, Meiting; Mei, Ye; Ryde, Ulf

Published in:
Journal of Chemical Theory and Computation

DOI:
10.1021/acs.jctc.8b00685

2018

Document Version:
Peer reviewed version (aka post-print)

Predicting Relative Binding Affinity Using Non-equilibrium QM/MM Simulations

Meiting Wang,[†,‡] Ye Mei,[*,†,¶] and Ulf Ryde[*,‡]

†*State Key Laboratory of Precision Spectroscopy, School of Physics and Materials Science, East China Normal University, Shanghai 200062, China*

‡*Department of Theoretical Chemistry, Lund University, Chemical Centre, P.O. Box 124, SE-221 00 Lund, Sweden*

¶*NYU-ECNU Center for Computational Chemistry at NYU Shanghai, Shanghai 200062, China*

E-mail: ymei@phy.ecnu.edu.cn; ulf.ryde@teokem.lu.se

Abstract

Calculating binding free energies with quantum mechanical (QM) methods is notoriously time consuming. In this work, we study whether such calculations can be accelerated by using non-equilibrium (NE) molecular dynamics simulations employing Jarzynski's equality. We study the binding of nine cyclic carboxylate ligands to the octa-acid deep-cavity host from the SAMPL4 challenge with the reference-potential approach. The binding free energies were first calculated at the molecular-mechanics (MM) level with free-energy perturbation, using the generalised Amber force field with restrained electrostatic-potential charges for the host and the ligands. Then, the free-energy corrections for going from the MM Hamiltonian to a hybrid QM/MM Hamiltonian were estimated by averaging over many short NE molecular dynamics simulations. In the QM/MM calculations, the ligand is described at the semiempirical PM6-DH+ level. We show that this approach yields MM→QM/MM free energy corrections that agree with those from other approaches within statistical uncertainties. The desired precision can be obtained by running a proper number of independent NE simulations. For the systems studied in this work, a total simulation length of 20 ps was appropriate for most ligands and 36–324 simulations were necessary in order to reach a precision of 0.3 kJ/mol.

Introduction

Accurate predictions of the binding affinities for small molecules to biological macromolecules is critical in computational structure-based drug design and is one of the essential challenges of computational chemistry.[1–3] In order to make these calculations more feasible, numerous free energy calculation methods have been suggested over the past few decades.[4,5] According to large-scale benchmark tests, alchemical free-energy perturbation (FEP) calculations yield rather accurate predictions of relative binding free energies for many protein–ligand complexes, with a mean absolute deviation of 4–6 kJ/mol. But for some proteins, the results are poor.[6–8] The accuracy of such calculations are in principle limited only by the amount of sampling (length of the simulation) and the accuracy of the energy function, which normally is a nonpolarizable force field.[9–12]

However, nonpolarizable force fields lack an explicit description of electronic response to the specific chemical environment and the predictive capability of force fields is limited.[13,14] On the other hand, quantum mechanical (QM) methods can provide an accurate description of the potential energy surface. Unfortunately, full QM calculations of protein-ligand binding affinity are not feasible due to the steep computational scaling of CPU time and memory requirement. Even with the hybrid QM/MM scheme,[15–20] in which the environment is treated at MM level, it is still very expensive to generate ensembles of structures for a free energy calculation.

The free-energy difference between two states is independent of the path of transformation. Therefore, there has been much interest in the reference-potential scheme recently. It was pioneered by Gao, Warshel and co-workers,[21–25] followed by implementations and enhancement by many other groups.[26–35] These methods are based on the thermodynamic cycle shown in Fig. 1. A direct computation of the QM/MM free energy difference $\Delta G^{\mathrm{QM/MM}}_{\mathrm{L_0}\rightarrow\mathrm{L_1}}$ between ligands $\mathrm{L_0}$ and $\mathrm{L_1}$ (the dashed arrow in Fig. 1) is usually unaffordable. Instead, it can be computed via an FEP calculation at the MM level ($\Delta G^{\mathrm{MM}}_{\mathrm{L_0}\rightarrow\mathrm{L_1}}$; the bottom arrow in Fig. 1), followed by two additional FEP calculations that convert the MM Hamiltonian to

the QM/MM Hamiltonian for the ligands (the vertical arrows in Fig. 1).[23,27,36] The free energy difference between the MM and QM/MM Hamiltonians can be obtained by single-step exponential averaging (ssEA)[27,33,34] and non-Boltzmann Bennett (NBB) calculations.[32,37] Thereby, sampling at the QM/MM level of theory can be avoided.

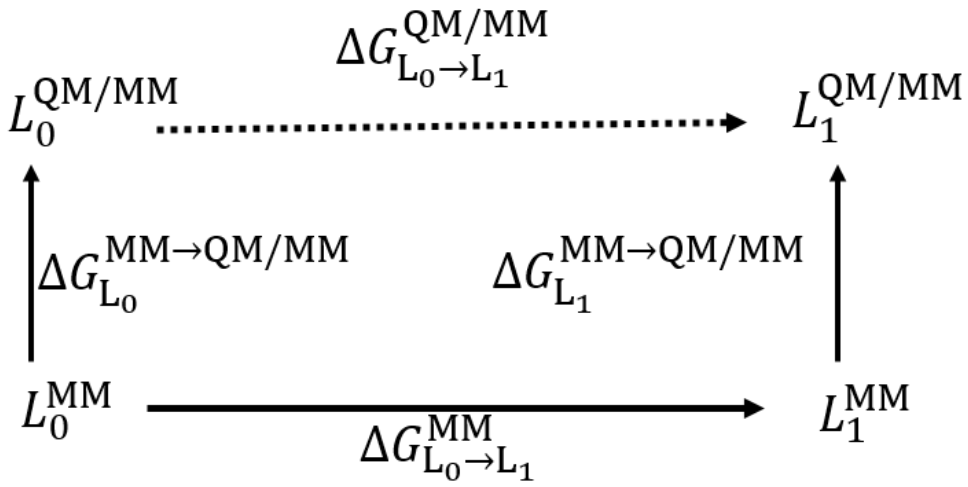

Figure 1: The reference-potential approach

The prime problem with these approaches is the slow convergence of the free energy difference.[34,36,38] For instance, the ssEA approach has been shown to give accurate results with low computational effort.[33,39] However, to obtain converged results for the MM→QM/MM perturbation in a host–guest binding system, ∼700 000 QM calculations were needed and it was necessary to use a cumulant approximation employing interaction energies (and there were indications that the calculations were still not fully converged).[27] FEP methods yield accurate results only when the two states are similar enough so that there is sufficient phase-space overlap (i.e. conformations with a large probability in one state also have a high probability to be sampled in the other state). To mitigate this difficulty, FEP calculations are often strengthened by stratification, in which a series of intermediate states are introduced. However, the sampling of the intermediate states require energy and force evaluations at the QM/MM level, making this MM→QM/MM perturbation very demanding.

To solve this problem, Ryde et al. have proposed two alternative approaches: reference-potential calculations with QM/MM sampling (RPQS)[28] and reference-potential calculations

with QM/MM sampling and many short simulations (RPQS-MSS).[40] As the names indicate, both methods require expensive QM/MM sampling. These two methods yielded the same results and both of them are more efficient than a direct QM/MM FEP calculation (the dashed arrow in Fig. 1).[28] In the RPQS approach, some intermediate states were introduced to gradually convert the MM Hamiltonian to the QM/MM Hamiltonian. Therefore, the RPQS approach is much more demanding than ssEA calculations. To enhance the efficiency, multiple short MD simulations were employed in the RPQS-MSS scheme, exploiting the fact that the phase space is already thoroughly sampled at the MM level.[40] With such an approach, the QM/MM simulation time could be reduced by a factor of four.

Recently, several studies have shown that non-equilibrium (NE) simulations[41–49] can be used to calculate the potential of mean force (PMF) along a reaction coordinate[50–53] and can also be used to estimate binding free energies via alchemical transformations.[54,55] NE simulations can also be used to estimate the free energy change associated to the MM→QM/MM process, which is a special case of an alchemical transformation.[56–59] In such simulations, energy and force evaluations with a QM/MM Hamiltonian are still inevitable, but the number of energy and force evaluations can be significantly less than that in a direct equilibrium free energy calculation at the same level.[45] Moreover, the NE free-energy calculations are trivially parallel, which further enhances the efficiency.

NE simulations also employ many short simulations to estimate free energies. Therefore, it is of great interest to compare the efficiency of the RPQS-MSS and NE methods in the calculations of QM/MM binding free energies. In this work, the relative free energies for the binding of nine cyclic carboxylate ligands to the octa-acid deep-cavity host, were calculated at the QM/MM level with the reference-potential approach. Non-equilibrium MD simulations were used to estimate the MM→QM/MM free energies. The results are compared to our previous studies of the same systems with the QM/MM FEP, RPQS and RPQS-MSS approaches[27,28,40] to decide which method is the most efficient.

Method

The Reference-Potential Approach

In this work, the relative binding free energies of nine cyclic carboxylate ligands to the octa-acid deep-cavity cavitand were studied, which were taken from the SAMPL4 competition.[60,61] The octa-acid host and nine guest molecules are shown in Fig. 2. Eight ligand transformations were considered in this study, viz. MeBz → Bz, EtBz → MeBz, pClBz → Bz, mClBz → Bz, Hx → Bz, MeHx → Hx, Hx → Pen, and Hep → Hx.

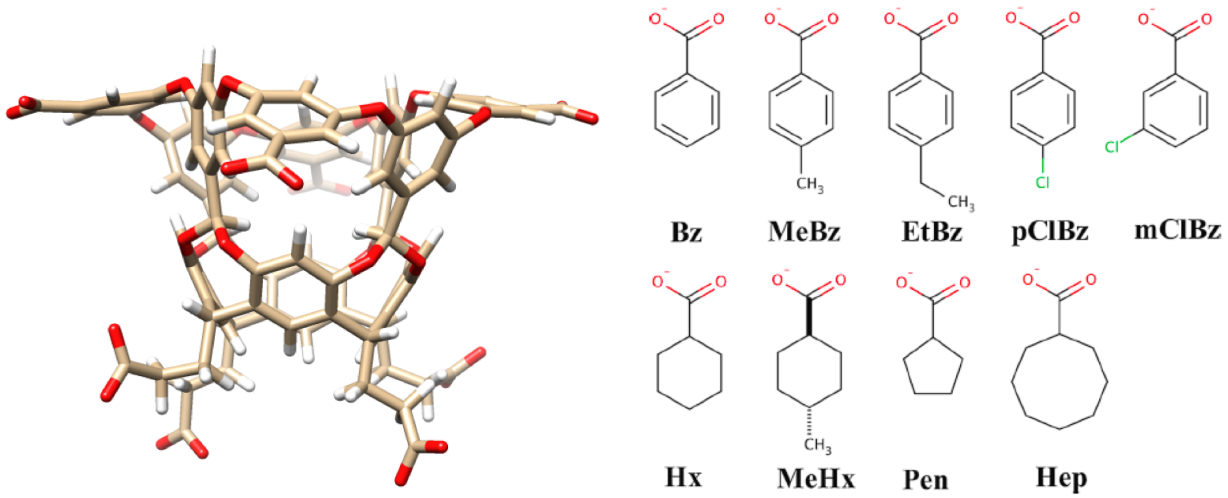

Figure 2: The octa-acid host and the nine guest molecules studied in this work.

QM/MM relative binding free energies were obtained with the reference-potential scheme shown in Fig. 1. With this thermodynamic cycle, the relative binding energies are first determined at MM level using FEP ($\Delta G^{\mathrm{MM}}_{\mathrm{L_0\rightarrow L_1,s}}$, where s refers to either the bound or the free state), employing a series of intermediate states. Then, the free energy differences between the MM and QM/MM Hamiltonians ($\Delta G^{\mathrm{MM\rightarrow QM/MM}}_{\mathrm{L_i,s}}$) are calculated for each ligand ($\mathrm{L_0}$ and $\mathrm{L_1}$). By combining the results from these three paths, the free energy difference at the QM/MM level is obtained:

$$\Delta G^{\mathrm{QM/MM}}_{\mathrm{L_0\rightarrow L_1,s}} = \Delta G^{\mathrm{MM}}_{\mathrm{L_0\rightarrow L_1,s}} - \Delta G^{\mathrm{MM\rightarrow QM/MM}}_{\mathrm{L_0,s}} + \Delta G^{\mathrm{MM\rightarrow QM/MM}}_{\mathrm{L_1,s}} \quad (1)$$

Finally, the net binding free energy is obtained by subtracting the free energy difference in the free state from that in the bound state:

$$\Delta G^{\mathrm{QM/MM}}_{\mathrm{L_0\rightarrow L_1}} = \Delta G^{\mathrm{QM/MM}}_{\mathrm{L_0\rightarrow L_1,bound}} - \Delta G^{\mathrm{QM/MM}}_{\mathrm{L_0\rightarrow L_1,free}} \tag{2}$$

In this paper, we will primarily discuss the MM→QM/MM free energies and in particular:

$$\Delta G^{\mathrm{MM\rightarrow QM/MM}}_{\mathrm{L_i}} = \Delta G^{\mathrm{MM\rightarrow QM/MM}}_{\mathrm{L_i,bound}} - \Delta G^{\mathrm{MM\rightarrow QM/MM}}_{\mathrm{L_i,free}} \tag{3}$$

The MM calculations are taken from our previous studies on the same systems.[36] In these simulations, the general Amber force field (GAFF)[9] was applied for both the host and the guest molecules and the partial charges of the system were obtained by the restrained electrostatic potential (RESP)[62,63] charge fitting method, using the electrostatic potential computed at HF/6-31G* level of theory. Water molecules were modelled by the TIP3P potential.[64]

Non-Equilibrium Simulations

In this work, NE simulations were applied within the reference-potential with QM/MM sampling scheme to calculate the free energy difference between the MM and QM/MM Hamiltonians, an approach that will be denoted as RPQS-NE hereafter. In 1997, Jarzynski proved that an equilibrium free energy difference can be expressed as an exponential average of the work performed on the system during an irreversible transformation between two states,[41,42] viz.

$$\exp(-\beta\Delta G) = \langle \exp(-\beta W) \rangle \,. \tag{4}$$

Here, the angle brackets $\langle \cdots \rangle$ denote the average over an ensemble of N_{trj} non-equilibrium transformation processes initiated from equilibrium states and $\beta = 1/RT$, where R is the gas

constant and T is the absolute temperature ($T = 300$ K in this study). The non-equilibrium work W is accumulated as[43]

$$\begin{aligned} W(t+\delta t) =& W(t) + \delta W(t \rightarrow t+\delta t) \\ =& W(t) + U(\mathbf{r}(t), \lambda(t+\delta t)) - U(\mathbf{r}(t), \lambda(t)), \end{aligned} \tag{5}$$

where $W(t)$ and $W(t+\delta t)$ are the work done to the system at time t and $t+\delta t$, respectively, and δW is the work associated in switching the Hamiltonian from $H(\lambda(t))$ to $H(\lambda(t+\delta t))$ with the coordinates fixed at $\mathbf{r}(t)$. U is the potential energy of the system, which is a function of both the coordinates and λ. Thus, the work in the Eq. 4 can be obtained from

$$W = \sum_{t=0}^{\tau-\delta t} U(\mathbf{r}(t), \lambda(t+\delta t)) - U(\mathbf{r}(t), \lambda(t)). \tag{6}$$

If not otherwise stated, 100 independent NE simulations were used to calculate the free-energy difference between the MM and QM/MM Hamiltonians for each ligand, either bound to the receptor or free in the water (i.e. $N_{\mathrm{trj}} = 100$). The QM calculations were performed with the semiempirical PM6-DH+ method[65] and only the ligand was included in the QM region, whereas the host molecule was described with GAFF. The TIP3P water model was utilized for the solvent water molecules. The PM6-DH+ method was selected because our previous calculations were performed at this level of theory[28,40] and it is among the best semiempirical methods available in the Amber software. All simulations were carried out with the QM/MM approach[66] implemented in the sander module of the Amber14 software[67] using the dual-topology scheme.

The NE simulations were started from the coordinates and velocities saved during the production simulation in a canonical ensemble for the two end states at the MM level. The temperature was kept at 300 K using Langevin dynamics[68] and the pressure was set to 1 atm using Berendsen's barostat.[69] The nonbonded interactions were truncated in real space at 8.0 Å, but the long-range Coulomb interactions were calculated using the particle mesh

Ewald (PME) method.[70] No bond-length constraints were used and the time step in the simulations was 1 fs. For each NE simulation, the potential was changed from MM to QM/MM by employing the coupling parameter λ:

$$U(\lambda) = (1-\lambda)U_{\mathrm{MM}} + \lambda U_{\mathrm{QM/MM}} \tag{7}$$

If not otherwise stated, in each simulation, λ changes from 0 to 1 in 200 stages with an interval of 0.1 ps between two adjacent jumps of λ. Therefore, the total simulation time for each trajectory was 20 ps. In Amber, this is determined by the parameters dynlmb = 0.005 and ntave = 100 (λ increases by 0.005 every 100 MD steps). These two parameters are denoted $\Delta\lambda$ and N_{ts} below.

Standard error and Convergence Criteria

The precision of the free energies from the NE simulation was estimated according to:[71]

$$\sigma^2 = \frac{1}{\beta^2 N_{\mathrm{trj}}} \left(\frac{\langle \exp(-\beta W)^2 \rangle}{\langle \exp(-\beta W) \rangle^2} - 1 \right). \tag{8}$$

It was estimated by numerically stable algorithms to avoid overflow and rounding errors. We have confirmed that bootstrapping gives the same standard error within 0.1 kJ/mol (cf. Table S1).

To study the convergence of the MM→QM/MM free-energy difference, five criteria were employed. The first is the standard deviation of the energy difference distribution σ, recommended by Ryde.[72] The second one is the reweighting entropy S_w:[34]

$$S_w = -\frac{1}{\ln N_{\mathrm{trj}}} \sum_{j=1}^{N_{\mathrm{trj}}} w_j \ln w_j, \tag{9}$$

where

$$w_j = \frac{\exp(-\beta W_j)}{\sum_{i=1}^{N_{\mathrm{trj}}} \exp(-\beta W_i)} \tag{10}$$

is the weight of each term in the average on the right-hand side of Eq. 4. The third one is the maximum value of these weights, $w_{\max}$, which provides the largest contribution to the exponential average. The fourth one is the Kish's effective sampling size, which is defined as

$$Q = \frac{(\sum_{j=1}^{N_{\mathrm{trj}}} w_j)^2}{\sum_{j=1}^{N_{\mathrm{trj}}} w_j^2}. \tag{11}$$

To make it independent of the actual number of samples, $Q' = Q/N_{\mathrm{trj}}$ was used. The last one is Wu and Kofke's bias metrics (Π), which can be calculated from[73]

$$\Pi = \sqrt{W_{\mathrm{L}}[\frac{1}{2\pi(N_{\mathrm{trj}}-1)^2}]} - \sqrt{2\beta(< w > -\Delta G)}. \tag{12}$$

where $W_{\mathrm{L}}(x)$ is the Lambert W function.

Results and Discussion

We have studied whether non-equilibrium MD simulations with Jarzynski's equality can be employed to calculate accurate QM/MM binding free energies. Towards this end, we have studied the binding of nine cyclic carboxylate ligands to the octa-acid deep-cavity host.[60,61] We used the semiempirical PM6-DH+ method for the ligand,[65] the GAFF force field for the host[9] and TIP3P for water molecules.[64] We have studied this system with several other QM/MM-FEP approaches before (ssEA, full QM/MM-FEP, RPQS and RPQS-MSS),[27,28,40] giving firm reference values and allowing us to discuss the efficiency of the various methods. The RPQS calculations employed the same thermodynamic cycle as the present RPQS-NE simulations (Fig. 1), but calculated the $\Delta G_{\mathrm{L,free}}^{\mathrm{MM}\rightarrow\mathrm{QM/MM}}$ free energy by FEP and 4–9 Λ values,

employing 1.5 ns QM/MM MD simulations for each Λ value. RPQS-MSS used 4 Λ values and run 5–43 simulations of 4×20 ps to reach a precision of 0.3 kJ/mol.

Parameters for the NE simulations

Optimal control parameters for the NE simulations need to be determined in the first place. To this end, the MM $\rightarrow$ QM/MM free energy difference of MeBz in the free state was studied. This molecule was chosen because it showed a quite slow convergence in our previous study.[40] As mentioned in the Method section, the accuracy and time-consumption of the NE simulations depend on three parameters: the number of the NE simulations to compute the average (N_{trj}), the number of MD steps between each jump in λ (N_{ts}) and the change of λ in each jump ($\Delta\lambda$). Thus, the total number of different λ values used is $1/\Delta\lambda$ and considering that we used a time step of 1 fs, the total time for each individual simulation in the ensemble is $\frac{N_{\mathrm{ts}}}{1000\times\Delta\lambda}$ picoseconds (ps). As will be discussed further below, we use N_{trj} to obtain the desired precision of the calculated free energies, but proper values of the other two parameters need to be determined.

Some initial test calculations (cf. the Supporting Information) showed that simulations with $\Delta\lambda = 0.01$ and 0.005 gave a proper compromise between accuracy and time consumption. The results of these two choices for $\Delta\lambda$ are presented in Fig. 3 with varying N_{ts} (100–500) and N_{trj} (10–100). The reference values (full line in the figure) were obtained from our previous study with full RSQS and four Λ values.[28] It can be seen that all estimated $\Delta G^{\mathrm{MM}\rightarrow\mathrm{QM/MM}}_{\mathrm{MeBz,free}}$ have converged to within 1 kJ/mol (shown in dashed lines) of the reference value (shown in full line) when N_{trj} is large enough. This convergence limit was also employed in our previous RPQS-MSS study and represents both a reasonable level of accuracy and an approximate 95% confidence interval for the difference between the RPQS and RPQS-NE results.[40] However, the standard error (SE) of the shortest simulation, 0.01–100 (i.e. with $\Delta\lambda = 0.01$ and $N_{\mathrm{ts}} = 100$, shown in black) is larger than that of the reference simulation (0.3 kJ/mol, cf. Fig. 3b and it does not show the expected $1/\sqrt{N_{\mathrm{trj}}}$ behaviour).

The second-shortest simulations are the 0.01–200 and 0.005–100 combinations, shown in red in Fig. 3. Both simulations give converged $\Delta G^{\mathrm{MM}\rightarrow\mathrm{QM/MM}}_{\mathrm{MeBz,free}}$, but the SE is lower and the convergence is faster for the 0.005–100 simulation (the 0.01–200 simulation requires 60 trajectories before the SE is below 0.3 kJ/mol). It can also be seen that the results are well converged compared to simulations using longer simulations (green, yellow and blue curves in Fig. 3). Therefore, the combination of $\Delta\lambda = 0.005$ and $N_{\mathrm{ts}} = 100$ was chosen for the calculations with the other ligands in this study.

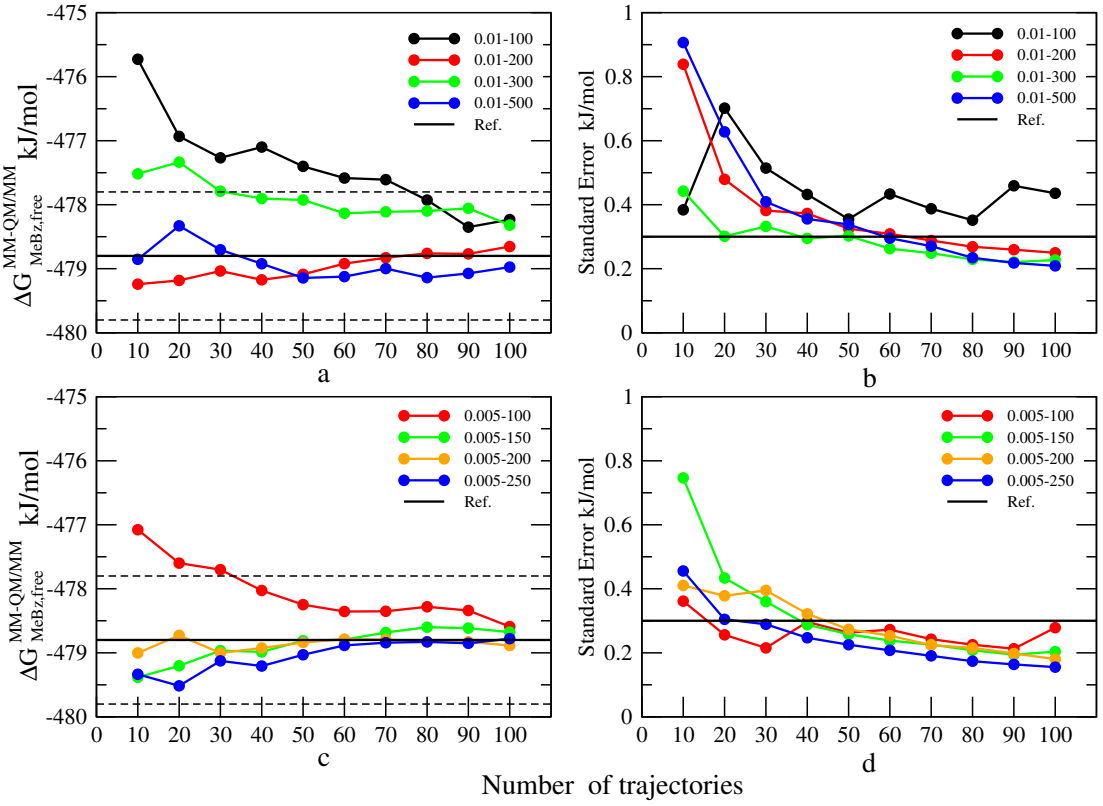

Figure 3: Convergence of $\Delta G^{\mathrm{MM}\rightarrow\mathrm{QM/MM}}_{\mathrm{MeBz,free}}$ (a and c) and the standard error (b and d) with respect to N_{trj} for different values of $\Delta\lambda$ (0.01 in a and b or 0.005 in c and d) and N_{ts} (for each curve, the legend indicates $\Delta\lambda$–N_{ts}). Note that curves with the same colour have the same total length of the simulation. Black dotted lines denote the ±1 kJ/mol deviation from the reference value for $\Delta G^{\mathrm{MM}\rightarrow\mathrm{QM/MM}}_{\mathrm{MeBz,free}}$ (shown in a black full line).

Convergence of $\Delta G_{L,s}^{\mathrm{MM}\rightarrow\mathrm{QM/MM}}$ with respect to the number of trajectories N_{trj}

Next, we studied how $\Delta G_{\mathrm{L,free}}^{\mathrm{MM}\rightarrow\mathrm{QM/MM}}$ and $\Delta G_{\mathrm{L,bound}}^{\mathrm{MM}\rightarrow\mathrm{QM/MM}}$ converge with respect to the number of NE trajectories N_{trj} (using $\Delta\lambda = 0.005$ and $N_{\mathrm{ts}} = 100$) for all the ligands. The results are shown in Fig. 4.

As shown in Fig. 4a, all $\Delta G_{\mathrm{L,free}}^{\mathrm{MM}\rightarrow\mathrm{QM/MM}}$ for the free ligands in water converged to the reference values within 1 kJ/mol. For Bz, Hx, Pen and Hep, the results are converged already with ten NE trajectories and for the other five guest molecules (MeBz, EtBz, pClBz, mClBz and MeHx), 20–40 trajectories are required to yield converged result. With 100 NE trajectories, $\Delta G_{\mathrm{L,free}}^{\mathrm{MM}\rightarrow\mathrm{QM/MM}}$ agrees with the reference values within 0.5 kJ/mol for all the ligands except for pClBz and Hx (0.7 kJ/mol). Moreover, for most of the ligands, the SEs of the calculations are less than or equal to those of the reference simulation (listed in Table S1). Only for Bz and EtBz, the SEs are 0.1 kJ/mol larger than for the reference simulation. For MeBz, pClBz, Hx, MeHx and Hep, less than 30 trajectories are enough to yield the same SE as in the reference calculations.

When the guest molecules are bound to the host, $\Delta G_{\mathrm{L,bound}}^{\mathrm{MM}\rightarrow\mathrm{QM/MM}}$ converges with less than 10 trajectories for five ligands (Bz, pClBz, MeHx, Pen and Hep) as can be seen in Fig. 4b and Table S1. For Hx, the results converges with 20 trajectories, but for EtBz and MeBz 50 and 80 trajectories are required, respectively. However, the deviation from the reference values is somewhat larger for the bound state. Only for Hx, Pen and Hep, the difference is less than 0.5 kJ/mol with 100 trajectories. Nonetheless, the SEs of the bound state were no larger than in the reference simulations, except for mClBz. For Bz, MeBz, Hx, MeHx and Pen, 50 trajectories is enough to yield the same SE as in the reference.

However, $\Delta G_{\mathrm{mClBz,bound}}^{\mathrm{MM}\rightarrow\mathrm{QM/MM}}$ for mClBz does not converge to the reference value even after 100 trajectories. This ligand gave poor convergence also in our previous RPQS-MSS study[40] and we showed that the problem is caused by the fact that the preferred orientation of the chlorine atom in the host is different in the MM (to the side) and QM simulations (to the bottom of the host). Therefore, we carried out additional simulations, in which N_{ts} was

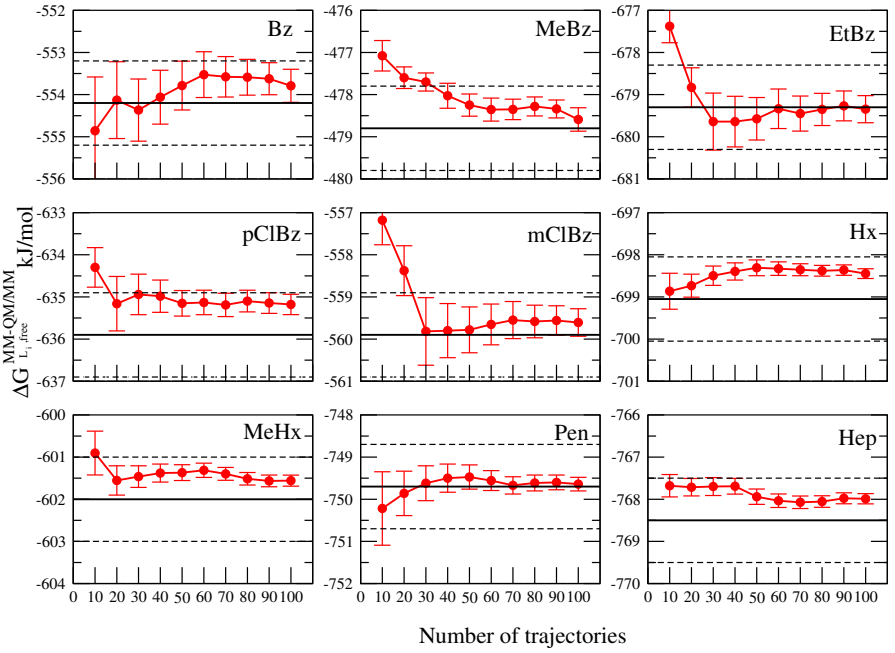

(a)

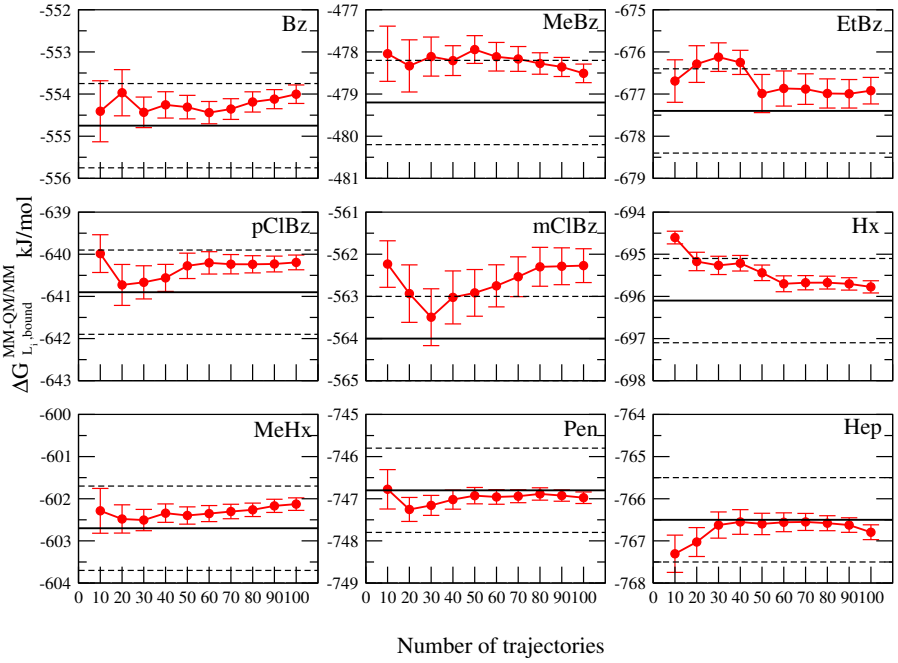

(b)

Figure 4: Convergence of (a) $\Delta G_{\mathrm{L,free}}^{\mathrm{MM\to QM/MM}}$ and (b) $\Delta G_{\mathrm{L,bound}}^{\mathrm{MM\to QM/MM}}$ as a function of N_{trj}. The RPQS results with 1.5 ns MD simulations for four Λ values are shown as black full lines with ± 1 kJ/mol marked in black dotted lines.

increased to 200, 500 and 1000. The results in Fig. 5 show that with $N_{\rm ts}$ = 200 (green line), $\Delta G^{\rm MM\rightarrow QM/MM}_{mClBz,bound}$ is still not converged, giving a final deviation from the reference by 1.6 kJ/mol. However, when $N_{\rm ts}$ increased to 500 (blue line), convergence within 1 kJ/mol is reached with 30 trajectories. Although the SE is 0.1 kJ/mol larger than the reference value with 100 trajectories, the result seems to be reliable. When $N_{\rm ts}$ was further increased to 1000, $\Delta G^{\rm MM\rightarrow QM}_{\rm mClBz,bound}$ converges to a constant value deviating by only 0.5 kJ/mol from the reference with only 40 trajectories and the SE decreases to 0.2 kJ/mol after 100 trajectories, which is lower than for the reference calculation.

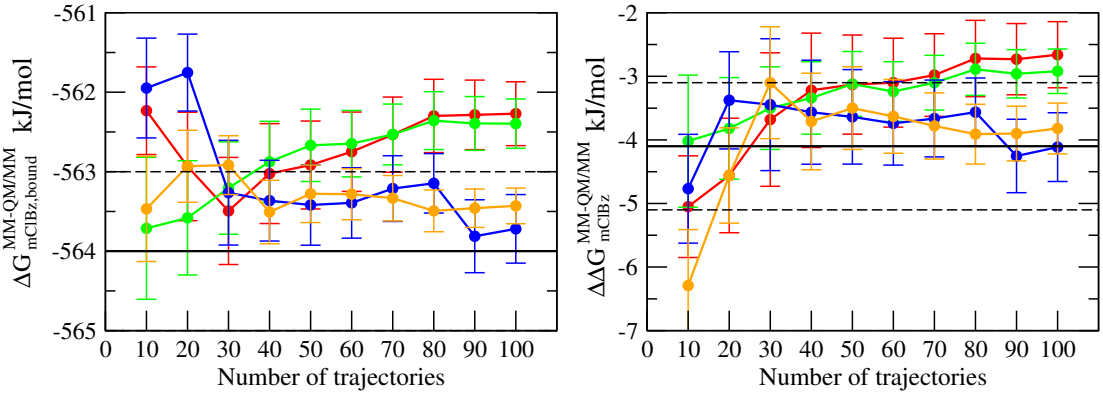

Figure 5: (a) $\Delta G^{\rm MM\rightarrow QM/MM}_{\rm mClBz,bound}$ and (b) $\Delta\Delta G^{\rm MM\rightarrow QM/MM}_{\rm mClBz}$ for the mClBz ligand with $N_{\rm ts}$=100 (red), 200 (green), 500 (blue), and 1000 (yellow). The reference values are shown as black full lines and the error bars represent the standard errors in the calculations.

Finally, the net $\Delta G^{\rm MM\rightarrow QM/MM}_{L_i}$ was computed by combining the results for each ligand in the bound and the free states, according to Eq. 3. As shown in Fig. 6 and Table 1, the results converged to within 1 kJ/mol from the reference values for all of the nine guest molecules with 10–50 trajectories. Even with 40 trajectories, seven of the nine ligands (except for EtBz and Hep) have converged and the deviations from the reference values are not greater than 0.5 kJ/mol. For most ligands, the SE is lower than in the RPQS study after 20 (Hx and Hep) to 70 (MeBz) trajectories, but for Bz, EtBz and mClBz, the SE is slightly larger than 0.5 kJ/mol even with 100 trajectories.

We have tried to use five convergence criteria (σ, S_w, $w_{\rm max}$, Q' and Π) to decide proper values of the $\Delta\lambda$ and $N_{\rm ts}$ parameters. However, as is discussed in the Supporting Information,

it was hard to find conclusive criteria that work for all systems and give reliable trends for variations in $\Delta\lambda$ and N_{ts}, although $\sigma < 0.8\ RT$, $S_w > 0.9$, $Q' > 0.4$ and $\Pi > 1.3$ may give some indication that the parameters are properly selected.

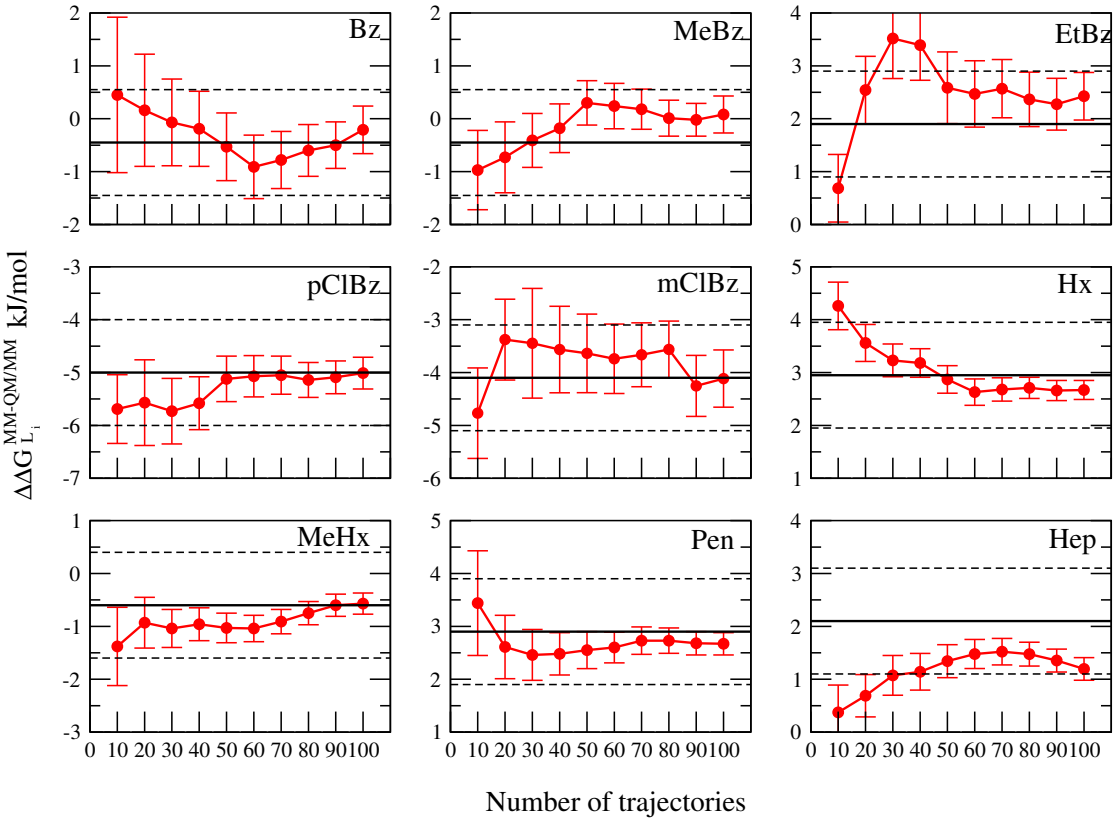

Figure 6: Convergence of $\Delta G_{\mathrm{L}}^{\mathrm{MM}\rightarrow\mathrm{QM/MM}}$ as a function of N_{trj}. The results were obtained with $\Delta\lambda = 0.005$ and $N_{\mathrm{ts}} = 100$, except for mClBz ($\Delta\lambda = 0.005$ and $N_{\mathrm{ts}} = 500$). RPQS results with four Λ values[28] are shown as a black full line with ± 1 kJ/mol marked in dashed lines.

Table 1: Calculated $\Delta G_{L_i}^{\mathrm{MM}\rightarrow\mathrm{QM/MM}}$ with standard errors (kJ/mol). For comparison, the RPQS results obtained with four Λ values are also shown. The last three rows indicate the number of trajectories needed to reach certain precisions.

N_{trj}	Bz	MeBz	EtBz	pClBz	mClBz	Hx	MeHx	Pen	Hep
10	0.45±1.47	-0.97±0.75	0.69±0.64	-5.69±0.65	-4.77±0.86	4.26±0.45	-1.38±0.74	3.44±0.99	0.37±0.52
20	0.16±1.06	-0.73±0.67	2.54±0.64	-5.57±0.81	-3.38±0.76	3.56±0.35	-0.93±0.48	2.61±0.60	0.69±0.40
30	-0.07±0.82	-0.41±0.51	3.52±0.76	-5.73±0.62	-3.45±1.03	3.23±0.31	-1.04±0.36	2.46±0.48	1.07±0.38
40	-0.19±0.71	-0.18±0.46	3.39±0.66	-5.58±0.50	-3.56±0.82	3.18±0.27	-0.96±0.31	2.48±0.40	1.14±0.35
50	-0.53±0.64	0.30±0.42	2.59±0.68	-5.12±0.43	-3.64±0.74	2.87±0.26	-1.03±0.28	2.55±0.35	1.34±0.31
60	-0.91±0.60	0.24±0.43	2.47±0.63	-5.07±0.39	-3.74±0.66	2.63±0.25	-1.04±0.25	2.60±0.29	1.48±0.28
70	-0.78±0.54	0.18±0.38	2.57±0.55	-5.05±0.36	-3.66±0.60	2.68±0.22	-0.91±0.23	2.73±0.26	1.52±0.25
80	-0.60±0.49	0.01±0.34	2.37±0.52	-5.14±0.33	-3.56±0.54	2.71±0.20	-0.75±0.22	2.73±0.24	1.47±0.23
90	-0.50±0.44	-0.02±0.31	2.27±0.49	-5.09±0.31	-4.25±0.58	2.66±0.19	-0.60±0.21	2.68±0.22	1.35±0.22
100	-0.21±0.45	-0.08±0.35	2.43±0.45	-5.01±0.30	-4.11±0.54	2.67±0.18	-0.57±0.20	2.67±0.21	1.19±0.21
ref.[a]	-0.53±0.38	-0.46±0.38	1.94±0.38	-5.03±0.35	-4.11±0.43	2.95±0.35	-0.63±0.34	2.89±0.34	2.06±0.35
N_{MSS}^{b}	38	25	24	18		9	13	6	13
N_{ref}^{c}	139	86	143	74	159	26	36	38	36
$N_{0.3}^{d}$	225	136	225	100	324	36	44	49	49

[a] Ref. 28.

[b] Number of trajectories needed to reach a standard error of 0.3 kJ/mol with RPQS-MSS.[40]

[c] Estimated number of trajectories needed to reach the same standard error as in the reference.

[d] Estimated number of trajectories needed to reach a standard error of 0.3 kJ/mol.

Efficiency

As shown in the previous section, the RPQS-NE method gives the same binding free energies (within statistical uncertainty) as those obtained in our previous RPQS and RPQS-MSS studies of the same systems,[28,40] which is quite satisfactory. Therefore, the next interesting question is which of the methods is the most efficient, i.e. which one requires the smallest computational effort. To that end, we compare the calculations that give the same precision (because for all the methods, the precision can be improved by running more or longer trajectories). For the RPQS and RPQS-NE methods, the SEs are shown in Table 1. In the penultimate row, the number of NE trajectories needed to reach the same SE as in the RPQS trajectories is given (N_{ref}), estimated from the SE with 100 trajectories and assuming a square-root dependence. It can be seen that 26–159 trajectories are needed, in total 736 trajectories for the nine ligands. Considering that the length of each simulation is 20 ps (100 ps for mClBz), the total simulation time for the nine ligands is 27.4 ns (in fact, the total simulation time is twice as long, because trajectories are needed both for the free and bound state). This should be compared to the RPQS calculations, which require $9 \times 4 \times 1.5 = 54$ ns (nine ligands, 4 λ values and 1.5 ns for each simulation). Thus, the RPQS-NE calculations are twice as effective as the original RPQS calculations. Moreover, excluding the problematic mClBz ligand (which requires the largest number of trajectories, each five times longer than for the other ligands), the RPQS-NE calculations are four times more efficient.

For the RPQS-MSS calculations, we aimed at an SE of 0.3 kJ/mol (OPT1 in ref. 40). The second last row in Table 2 shows the number of NE trajectories needed to obtain a SE of 0.3 kJ/mol ($N_{0.3}$, estimated in the same way). It can be seen that 36–225 NE trajectories are needed (excluding mClBz, which was not considered in ref. 40), giving a sum of 865 trajectories and a total length of 17.3 ns. For the corresponding RPQS-MSS calculations, only 145 trajectories were needed to reach a the same SE (N_{MSS} shown in the last row in Table 2), but each of them had a length of $4 \times 20 = 80$ ps (four Λ values, each with 20 ps simulation), giving a total of 11.6 ns. This indicates that the RPQS-NE approach is actually 1.5 times

more expensive than the RPQS-MSS calculations. Looking at the individual trajectories, RPQS-NE is more efficient for the MeHx and Hep ligands (by a factor of 1.1–1.2), whereas it is less efficient for the other ligands, with the largest difference for EtBz (a factor of 2.3).

Conclusions

We have investigated whether QM/MM calculations of binding free energies can be accelerated by the reference-potential approach using NE simulations and Jarzynski's equality to calculate the MM→QM/MM free-energy correction. We studied the binding of nine cyclic carboxylate ligands to the octa-acid deep-cavity host, taken from the SAMPL4 challenge,[60,61] which have been studied by Ryde et al. with many methods before, including MM-FEP, direct QM/MM-FEP, ssEA, NBB, RPQS and RPQS-MSS.[27,28,36,40] The MM calculations were run with the GAFF force field, whereas the ligand was treated by the semiempirical PM6-DH+ method in the QM/MM calculations.

By comparing to the QM/MM-FEP, RPQS and RPQS-MSS results (which were run with the same QM/MM approach), we can confirm that the present RPQS-NE approach gives MM→QM/MM free-energy corrections that agree with the previous results within the statistical uncertainty, i.e. ∼1 kJ/mol (the mean absolute deviation to the reference RPQS results with four Λ values is 0.4 kJ/mol). Thus, we have shown that RPQS-NE is an accurate approach for the calculation of QM/MM binding free energies.

Both RPQS-MSS and RPQS-NE are rigorous methods in that when provided with enough sampling, equilibration and λ values they give the correct results. However, if the number of simulations, the simulation length and the number of λ values or the rate of change in λ are too small, both methods become less accurate. We found that 4.3 ns QM/MM NE trajectories were required per ligand on average to reach a precision of 0.3 kJ/mol. This is 1.5 times more than for RPQS-MSS, so at least for these systems, there does not seem to be any advantage of running NE trajectories rather than many short equilibrium trajectories.

However, there may very well be other systems for which the situation is different.

Acknowledgement

U.R. is supported by grants from the Swedish research council (project 2014-5540) and from Knut and Alice Wallenberg Foundation (KAW 2013.0022). M.W. is supported by a scholarship from China Scholarship Council. Y.M. is supported by the National Natural Science Foundation of China (Grant No. 21773066) and the Fundamental Research Funds for the Central Universities. The computations were performed on computer resources provided by the Swedish National Infrastructure for Computing (SNIC) at Lunarc at Lund University.

Supporting Information Available

Results for $\Delta G_{\mathrm{L,free}}^{\mathrm{MM}\rightarrow\mathrm{QM/MM}}$ and $\Delta G_{\mathrm{L,bound}}^{\mathrm{MM}\rightarrow\mathrm{QM/MM}}$. Convergence criteria obtained for $\Delta G_{\mathrm{MeBz,free}}^{\mathrm{MM}\rightarrow\mathrm{QM/MM}}$ with different values of N_{trj}. This information is available free of charge via the Internet at http://pubs.acs.org.

References

(1) Homeyer, N.; Stoll, F.; Hillisch, A.; Gohlke, H. Binding Free Energy Calculations for Lead Optimization: Assessment of Their Accuracy in an Industrial Drug Design Context. *J. Chem. Theory Comput.* **2014**, *10*, 3331–3344.

(2) Sliwoski, G.; Kothiwale, S.; Meiler, J.; Lowe, E. W. Computational Methods in Drug Discovery. *Pharmacol. Rev.* **2014**, *66*, 334–395.

(3) Liao, C.; Sitzmann, M.; Pugliese, A.; Nicklaus, M. C. Software and Resources for Computational Medicinal Chemistry. *Future Med. Chem.* **2011**, *3*, 1057–1085.

(4) Gohlke, H.; Klebe, G. Approaches to the Description and Prediction of the Binding Affinity of Small-Molecule Ligands to Macromolecular Receptors. *Angew. Chemi. Int. Ed.* **2002**, *41*, 2644–2676.

(5) Gilson, M. K.; Zhou, H.-X. Calculation of Protein–Ligand Binding Affinities. *Annu. Rev. Biophys. Biomol. Struct.* **2007**, *36*, 21–42.

(6) Wang, L.; Wu, Y.; Deng, Y.; Kim, B.; Pierce, L.; Krilov, G.; Lupyan, D.; Robinson, S.; Dahlgren, M. K.; Greenwood, J.; Romero, D. L.; Masse, C.; Knight, J. L.; Steinbrecher, T.; Beuming, T.; Damm, W.; Harder, E.; Sherman, W.; Brewer, M.; Wester, R.; Murcko, M.; Frye, L.; Farid, R.; Lin, T.; Mobley, D. L.; Jorgensen, W. L.; Berne, B. J.; Friesner, R. A.; Abel, R. Accurate and Reliable Prediction of Relative Ligand Binding Potency in Prospective Drug Discovery by Way of a Modern Free-Energy Calculation Protocol and Force Field. *J. Am. Chem. Soc.* **2015**, *137*, 2695–2703.

(7) Christ, C. D.; Fox, T. Accuracy Assessment and Automation of Free Energy Calculations for Drug Design. *J. Chem. Inf. Model.* **2014**, *54*, 108–120.

(8) Mikulskis, P.; Genheden, S.; Ryde, U. A Large-Scale Test of Free-Energy Simulation Estimates of Protein–Ligand Binding Affinities. *J. Chem. Inf. Model.* **2014**, *54*, 2794–2806.

(9) Wang, J.; Wolf, R. M.; Caldwell, J. W.; Kollman, P. A.; Case, D. A. Development and Testing of a General Amber Force Field. *J. Comput. Chem.* **2004**, *25*, 1157–1174.

(10) Jorgensen, W. L.; Tirado-Rives, J. The OPLS Potential Functions for Proteins, Energy Minimizations for Crystals of Cyclic Peptides and Crambin. *J. Am. Chem. Soc.* **1988**, *110*, 1657–1666.

(11) Vanommeslaeghe, K.; Hatcher, E.; Acharya, C.; Kundu, S.; Zhong, S.; Shim, J.; Darian, E.; Guvench, O.; Lopes, P.; Vorobyov, I.; Mackerell, A. D. CHARMM General

Force Field: A Force Field for Drug-like Molecules Compatible with the CHARMM All-atom Additive Biological Force Fields. *J. Comput. Chem.* **2010**, *31*, 671–690.

(12) Dodda, L. S.; Cabeza de Vaca, I.; Tirado-Rives, J.; Jorgensen, W. L. LigParGen Web Server: An Automatic OPLS-AA Parameter Generator for Organic Ligands. *Nucleic Acids Res.* **2017**, *45*, W331–W336.

(13) Jorgensen, W. L. Special Issue on Polarization. *J.Chem. Theory Comput.* **2007**, *3*, 1877–1877.

(14) Harder, E.; Anisimov, V. M.; Whitfield, T.; MacKerell, A. D.; Roux, B. Understanding the Dielectric Properties of Liquid Amides from a Polarizable Force Field. *J. Phys. Chem. B* **2008**, *112*, 3509–3521.

(15) Warshel, A.; Levitt, M. Theoretical Studies of Enzymic Reactions: Dielectric, Electrostatic and Steric Stabilization of the Carbonium Ion in the Reaction of Lysozyme. *J. Mol. Biol.* **1976**, *103*, 227–249.

(16) Gao, J.; ; Truhlar, D. G. Quantum Mechanical Methods for Enzyme Kinetics. *Annu. Rev. Phys. Chem.* **2002**, *53*, 467–505.

(17) Bakowies, D.; Thiel, W. Hybrid Models for Combined Quantum Mechanical and Molecular Mechanical Approaches. *J. Phys. Chem.* **1996**, *100*, 10580–10594.

(18) Brunk, E.; Rothlisberger, U. Mixed Quantum Mechanical/Molecular Mechanical Molecular Dynamics Simulations of Biological Systems in Ground and Electronically Excited States. *Chem. Rev.* **2015**, *115*, 6217–6263.

(19) Ryde, U. QM/MM Calculations on Proteins. *Meth. Enz.* **2016**, *577*, 119–158.

(20) Senn, H. M.; Thiel, W. QM/MM Methods for Biomolecular Systems. *Angew. Chem. Int. Ed.* **2009**, *48*, 1198–1229.

(21) Gao, J. Absolute Free Energy of Solvation from Monte Carlo Simulations Using Combined Quantum and Molecular Mechanical Potentials. *J. Phys. Chem.* **1992**, *96*, 537–540.

(22) Gao, J.; Xia, X. A Priori Evaluation of Aqueous Polarization Effects through Monte Carlo QM-MM Simulations. *Science* **1992**, *258*, 631–635.

(23) Luzhkov, V.; Warshel, A. Microscopic Models for Quantum Mechanical Calculations of Chemical Processes in Solutions: LD/AMPAC and SCAAS/AMPAC Calculations of Solvation Energies. *J. Comput. Chem.* **1992**, *13*, 199–213.

(24) Wesolowski, T.; Warshel, A. Ab initio Free Energy Perturbation Calculations of Solvation Free Energy Using the Frozen Density Functional Approach. *J. Phys. Chem.* **1994**, *98*, 5183–5187.

(25) Muller, R. P.; Warshel, A. Ab initio Calculations of Free Energy Barriers for Chemical Reactions in Solution. *J. Phys. Chem.* **1995**, *99*, 17516–17524.

(26) Rod, T. H.; Ryde, U. Quantum Mechanical Free Energy Barrier for an Enzymatic Reaction. *Phys. Rev. Lett.* **2005**, *94*, 138302.

(27) Olsson, M. A.; Söderhjelm, P.; Ryde, U. Converging Ligand-binding Free Energies Obtained with Free-energy Perturbations at the Quantum Mechanical Level. *J. Comput. Chem.* **2016**, *37*, 1589–1600.

(28) Olsson, M. A.; Ryde, U. Comparison of QM/MM Methods to Obtain Ligand-Binding Free Energies. *J.Chem. Theory Comput.* **2017**, *13*, 2245–2253.

(29) Beierlein, F. R.; Michel, J.; Essex, J. W. A Simple QM/MM Approach for Capturing Polarization Effects in Protein-ligand Binding Free Energy Calculations. *J. Phys. Chem. B* **2011**, *115*, 4911–4926.

(30) Cave-Ayland, C.; Skylaris, C.-K.; Essex, J. W. Direct Validation of the Single Step Classical to Quantum Free Energy Perturbation. *J. Phys. Chem. B* **2015**, *119*, 1017–1025.

(31) Genheden, S.; Cabedo Martinez, A. I.; Criddle, M. P.; Essex, J. W. Extensive All-atom Monte Carlo Sampling and QM/MM Corrections in the SAMPL4 Hydration Free Energy Challenge. *J. Comput.-Aided Mol. Des.* **2014**, *28*, 187–200.

(32) König, G.; Pickard, F. C.; Mei, Y.; Brooks, B. R. Predicting Hydration Free Energies with a Hybrid QM/MM Approach: An Evaluation of Implicit and Explicit Solvation Models in SAMPL4. *J. Comput.-Aided Mol. Des.* **2014**, *28*, 245–257.

(33) Jia, X.; Wang, M.; Shao, Y.; König, G.; Brooks, B. R.; Zhang, J. Z. H.; Mei, Y. Calculations of Solvation Free Energy through Energy Reweighting from Molecular Mechanics to Quantum Mechanics. *J. Chem. Theory Comput.* **2016**, *12*, 499–511.

(34) Wang, M.; Li, P.; Jia, X.; Liu, W.; Shao, Y.; Hu, W.; Zheng, J.; Brooks, B. R.; Mei, Y. Efficient Strategy for the Calculation of Solvation Free Energies in Water and Chloroform at the Quantum Mechanical/Molecular Mechanical Level. *J. Chem. Inf. Model.* **2017**, *57*, 2476–2489.

(35) Liu, W.; Jia, X.; Wang, M.; Li, P.; Wang, X.; Hu, W.; Zheng, J.; Mei, Y. Calculations of the Absolute Binding Free Energies for Ralstonia Solanacearum Lectins Bound with Methyl-α-L-Fucoside at Molecular Mechanical and Quantum Mechanical/Molecular Mechanical Levels. *RSC Adv.* **2017**, *7*, 38570–38580.

(36) Mikulskis, P.; Cioloboc, D.; Andrejić, M.; Khare, S.; Brorsson, J.; Genheden, S.; Mata, R. A.; Söderhjelm, P.; Ryde, U. Free-energy Perturbation and Quantum Mechanical Study of SAMPL4 Octa-acid Host–guest Binding Energies. *J. Comput.-Aided Mol. Des.* **2014**, *28*, 375–400.

(37) König, G.; Boresch, S. Non–Boltzmann Sampling and Bennett's Acceptance Ratio Method: How to Profit from Bending the Rules. *J. Comput. Chem.* **2011**, *32*, 1082–1090.

(38) Genheden, S.; Ryde, U.; Söderhjelm, P. Binding Affinities by Alchemical Perturbation Using QM/MM with a Large QM System and Polarizable MM Model. *J. Comput. Chem.* **2015**, *36*, 2114–2124.

(39) Dybeck, E. C.; König, G.; Brooks, B. R.; Shirts, M. R. Comparison of Methods to Reweight from Classical Molecular Simulations to QM/MM Potentials. *J. Chem. Theory Comput.* **2016**, *12*, 1466–1480.

(40) Steinmann, C.; Olsson, M. A.; Ryde, U. Relative Ligand-Binding Free Energies Calculated from Multiple Short QM/MM MD Simulations. *J. Chem. Theory Comput.* **2018**, *14*, 3228–3237.

(41) Jarzynski, C. Nonequilibrium Equality for Free Energy Differences. *Phys. Rev. Lett.* **1997**, *78*, 2690.

(42) Jarzynski, C. Equilibrium Free-Energy Differences from Nonequilibrium Measurements: A Master-Equation Approach. *Phys. Rev. E* **1997**, *56*, 5018.

(43) Crooks, G. Nonequilibrium Measurements of Free Energy Differences for Microscopically Reversible Markovian Systems. *J. Statis. Phys.* **1998**, *90*, 1481.

(44) Chelli, R.; Marsili, S.; Barducci, A.; Procacci, P. Generalization of the Jarzynski and Crooks Nonequilibrium Work Theorems in Molecular Dynamics Simulations. *Phys. Rev. E* **2007**, *75*, 050101.

(45) Goette, M.; Grubmüller, H. Accuracy and Convergence of Free Energy Differences Calculated from Nonequilibrium Switching Processes. *J. Comput. Chem.* **2009**, *30*, 447.

(46) Ytreberg, F. M.; Zuckerman, D. M. Single-Ensemble Nonequilibrium Path-Sampling Estimates of Free Energy Differences. *J. Chem. Phys.* **2004**, *120*, 10876.

(47) Nicolini, P.; Frezzato, D.; Chelli, R. Exploiting Configurational Freezing in Nonequilibrium Monte Carlo Simulations. *J. Chem. Theory Comput.* **2011**, *7*, 582.

(48) Spichty, M.; Cecchini, M.; Karplus, M. Conformational Free-Energy Difference of a Miniprotein from Nonequilibrium Simulations. *J. Phys. Chem. Lett.* **2010**, *1*, 1922.

(49) Li, P.; Jia, X.; Wang, M.; Mei, Y. Comparison of Accuracy and Convergence Rate between Equilibrium and Nonequilibrium Alchemical Transformations for Calculation of Relative Binding Free Energy. *Chin. J. Chem. Phys.* **2017**, *30*, 789–799.

(50) Ngo, V. A.; Kim, I.; Allen, T. W.; Noskov, S. Y. Estimation of Potentials of Mean Force from Nonequilibrium Pulling Simulations Using Both Minh-Adib Estimator and Weighted Histogram Analysis Method. *J. Chem. Theory Comput.* **2016**, *12*, 1000.

(51) Chelli, R.; Marsili, S.; Procacci, P. Calculation of the Potential of Mean Force from Nonequilibrium Measurements via Maximum Likelihood Estimators. *Phys. Rev. E* **2008**, *77*, 031104.

(52) Chelli, R.; Procacci, P. A Potential of Mean Force Estimator Based on Nonequilibrium Work Exponential Averages. *Phys. Chem. Chem. Phys.* **2009**, *11*, 1152.

(53) Nicolini, P.; Procacci, P.; Chelli, R. Hummer and Szabo-like Potential of Mean Force Estimator for Bidirectional Nonequilibrium Pulling Experiments/Simulations. *J. Phys. Chem. B* **2010**, *114*, 9546.

(54) Procacci, P.; Cardelli, C. Fast Switching Alchemical Transformations in Molecular Dynamics Simulations. *J. Chem. Theory Comput.* **2014**, *10*, 2813.

(55) Sandberg, R. B.; Banchelli, M.; Guardiani, C.; Menichetti, S.; Caminati, G.; Procacci, P. Efficient Nonequilibrium Method for Binding Free Energy Calculations in Molecular Dynamics Simulations. *J. Chem. Theory Comput.* **2015**, *11*, 423.

(56) Hudson, P. S.; Woodcock, H. L.; Boresch, S. Use of Nonequilibrium Work Methods to Compute Free Energy Differences Between Molecular Mechanical and Quantum Mechanical Representations of Molecular Systems. *J. Phys. Chem. Lett.* **2015**, *6*, 4850–4856.

(57) Kearns, F. L.; Hudson, P. S.; Boresch, S.; Woodcock, H. L. In *Computational Approaches for Studying Enzyme Mechanism Part A*; Voth, G. A., Ed.; Methods in Enzymology; Academic Press, 2016; Vol. 577; pp 75–104.

(58) Boresch, S.; Woodcock, H. L. Convergence of Single-Step Free Energy Perturbation. *Mol. Phys.* **2017**, *115*, 1200–1213.

(59) Kearns, F. L.; Hudson, P. S.; Woodcock, H. L.; Boresch, S. Computing Converged Free Energy Differences between Levels of Theory via Nonequilibrium Work Methods: Challenges and Opportunities. *J. Comput. Chem.* **2017**, *38*, 1376–1388.

(60) Muddana, H. S.; Fenley, A. T.; Mobley, D. L.; Gilson, M. K. The SAMPL4 Host–guest Blind Prediction Challenge: An Overview. *J. Comput. Aided Mol. Des.* **2013**, *28*, 319–325.

(61) Gibb, C. L. D.; Gibb, B. C. Binding of Cyclic Carboxylates to Octa-acid Deep-cavity Cavitand. *J. Comput. Aided Mol. Des.* **2014**, *28*, 319–325.

(62) Cieplak, P.; Cornell, W. D.; Bayly, C.; Kollman, P. A. Application of the Multimolecule and Multiconformational RESP Methodology to Biopolymers: Charge Derivation for DNA, RNA, and Proteins. *J. Comput. Chem.* **1995**, *16*, 1357–1377.

(63) Bayly, C. I.; Cieplak, P.; Cornell, W.; Kollman, P. A. A Well-behaved Electrostatic Potential Based Method Using Charge Restraints for Deriving Atomic Charges: The RESP Model. *J. Phys. Chem.* **1993**, *97*, 10269–10280.

(64) Jorgensen, W. L.; Chandrasekhar, J.; Madura, J. D.; Impey, R. W.; Klein, M. L. Comparison of Simple Potential Functions for Simulating Liquid Water. *J. Chem. Phy.* **1983**, *79*, 926–935.

(65) Korth, M. Third-Generation Hydrogen-Bonding Corrections for Semiempirical QM Methods and Force Fields. *J. Chem. Theory Comput.* **2010**, *6*, 3808–3816.

(66) Walker, R. C.; Crowley, M. F.; Case, D. A. The Implementation of a Fast and Accurate QM/MM Potential Method in AMBER. *J. Comput. Chem.* **2007**, *29*, 1019–1031.

(67) Case, D. A.; Berryman, J. T.; Betz, R. M.; Cerutti, D. S.; Cheatham, T. E., III; Darden, T. A.; Duke, R. E.; Giese, T. J.; Gohlke, H.; Goetz, A. W.; Homeyer, N.; Izadi, N.; Janowski, P.; Kaus, J.; Kovalenko, A.; Lee, T. S.; LeGrand, S.; Li, P.; Luchko, T.; Luo, R.; Madej, B.; Merz, K. M.; Monard, G.; Needham, P.; Nguyen, H.; Nguyen, H. T.; Omelyan, I.; Onufriev, A.; Roe, D. R.; Roitberg, A.; Salomon-Ferrer, R.; Simmerling, C. L.; Smith, W.; Swails, J.; Walker, R. C.; Wang, J.; Wolf, R. M.; Wu, X.; York, D. M.; Kollman, P. A. AMBER 2015, University of California, San Francisco. 2015.

(68) Pastor, R. W.; Brooks, B. R.; Szabo, A. An Analysis of the Accuracy of Langevin and Molecular Dynamics Algorithms. *Mol. Phys.* **1988**, *65*, 1409–1419.

(69) Berendsen, H. J. C.; Postma, J. P. M.; van Gunsteren, W. F.; DiNola, A.; Haak, J. R. Molecular Dynamics with Coupling to an External Bath. *J. Chem. Phys.* **1984**, *81*, 3684–3690.

(70) Darden, T.; York, D.; Pedersen, L. Particle Mesh Ewald: An N·log(N) Method for Ewald Sums in Large Systems. *J. Chem. Phys.* **1993**, *98*, 10089–10092.

(71) Paliwal, H.; Shirts, M. R. A Benchmark Test Set for Alchemical Free Energy Transformations and Its Use to Quantify Error in Common Free Energy Methods. *J. Chem. Theory Comput.* **2011**, *7*, 4115–4134.

(72) Ryde, U. How Many Conformations Need to Be Sampled to Obtain Converged QM/MM Energies? The Curse of Exponential Averaging. *J. Chem. Theory Comput.* **2017**, *13*, 5745–5752.

(73) Wu, D.; Kofke, D. A. Model for Small-sample Bias of Free-energy Calculations Applied to Gaussian-distributed Nonequilibrium Work Measurements. *J. Chem. Phys.* **2004**, *121*, 8742–8747.

This material is available free of charge via the Internet at `http://pubs.acs.org/`.

Graphical TOC Entry